IEEE Access
Multidisciplinary | Rapid Review | Open Access Journal

Received January 16, 2018, accepted February 10, 2018, date of publication February 15, 2018, date of current version March 15, 2018.

Digital Object Identifier 10.1109/ACCESS.2018.2806372

A Naturalness Preserved Fast Dehazing Algorithm Using HSV Color Space

TIANYU ZHANG[1], HAI-MIAO HU[1,2], AND BO LI[1,2]

[1]Beijing Key Laboratory of Digital Media, School of Computer Science and Engineering, Beihang University, Beijing 100191, China
[2]State Key Laboratory of Virtual Reality Technology and Systems, Beihang University, Beijing 100191, China

Corresponding author: Hai-Miao Hu (frank0139@163.com)

This work was supported in part by the National Key Research and Development Program under Grant 2016YFC0801003, in part by the National Natural Science Foundation of China under Grants 61772058 and 61421003, and in part by the Fundamental Research Funds for the Central Universities.

ABSTRACT Visibility of outdoor scenes is often degraded by haze. The atmosphere particles absorb and scatter the light, causing failure in various computer vision applications. In this paper, we propose a naturalness preserved fast dehazing algorithm using hue, saturation, and value (HSV) color space. First, we process hazy images in HSV color space instead of red, green, and blue (RBG) in order to preserve hue and reduce computational complexity. Second, we use the modified morphological opening operation for estimating the transmission map. In this way, the halo effects are greatly suppressed, and it costs less time than the specially designed filters. The experimental results demonstrate that the proposed algorithm can effectively remove haze. Also, our algorithm maintains naturalness by preserving hue and suppressing halo effects. Moreover, the computational complexity has been largely reduced, thus making our algorithm appropriate for real-time applications.

INDEX TERMS Dehazing, HSV color space, naturalness, opening operation.

I. INTRODUCTION

The visibility of images captured in outside scenes is debased or degraded by haze. Those images suffer from low contrast and color distortion, which hinders satisfactory performance in computer vision applications.

Many algorithms have been proposed to solve the image dehazing problem. The physical model widely used to describe the cause of formation of hazy images is the atmospheric scattering model [1]. Early algorithms focus on some priors due to the insufficient depth information. Tan [2] removes haze by maximizing hazy image contrast in local regions. Fattal [3] uses the assumption that the transmission and surface shading are locally uncorrelated to estimate the transmission map. In 2009, the dark channel prior (DCP) was proposed [4], which has been regarded as the state-of-the-art. Nevertheless, the algorithm proposed in [4] cannot preserve the color and may bring halo effect in complex structures. As a result, dehazed images will suffer from color shift and artifact effects [5].

He *et al.* [6] propose using guided filtering instead of soft matting to refine transmission map. It improves time efficiency, but the estimation of the transmission map is not abundant because the guided filter is only an approximation of soft matting. Zhang *et al.* [7] replace minimum operator by median operator. The dark channels become less blurry, but the median-based algorithm is less physically meaningful.

Recently, algorithms based on machine learning have been proposed. Zhu *et al.* [8] use color attenuation prior (CAP) to estimate the scene depth. A learning strategy is applied to calculate the parameters. This algorithm has limited applicability due to insufficient prior information. Cai *et al.* [9] introduce deep learning to image dehazing. It is the first deep learning algorithm for dehazing, but their algorithm is time-consuming and tends to keep more haze in dehazing results. Jiang *et al.* [10] use a surrogate-based algorithm to learn a refined polynomial regression model for optical depth. The depth has errors because the regression model cannot fit all scene points.

Currently, the dehazing algorithms still have problems on computation complexity or deficient results. The naturalness of images are ruined by halo effects or color distortion due to imperfect priors. Many specially-designed filters are proposed to refine the coarse results, thus making the whole process time-consuming. According to our previous works [11], [12], naturalness and processing speed is important for single image dehazing.

To address the problems of the loss of naturalness and reduce the time expenses, we propose a naturalness

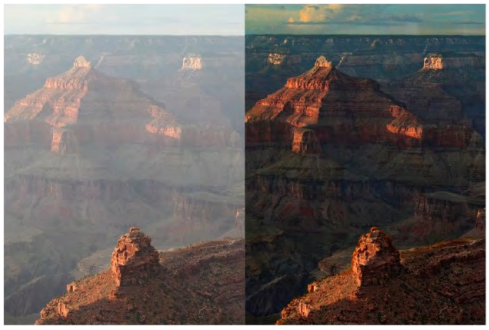

(a)

(b)

FIGURE 1. Hazy images and results of our proposed algorithm.

preserved fast dehazing algorithm using HSV color space. First, by processing hazy images in HSV color space instead of RGB, we can preserve hue and reduce computational complexity. Second, we use the modified morphological opening operation for the estimation of the transmission map. In this way, the halo effects are greatly suppressed and it costs less time than the specially-designed filters. The experimental results demonstrate that the proposed algorithm can effectively remove haze. Also, our algorithm maintains naturalness by preserving hue and suppressing halo effects (see Fig.1). Moreover, the computational complexity has been largely reduced, thus making our algorithm appropriate for real-time applications.

II. PROPOSED ALGORITHM

A. OBSERVATIONS OF HSV COLOR SPACE

Hue, Saturation and Value (HSV) color space is related with human vision. Wan and Chen [13] prove the hue channel of hazy image is invariant under certain circumstances. This feature inspires us to recover hazy images by dealing with the brightness and the saturation. The conversion from RGB to HSV is as follows:

$$H' = \begin{cases} 0 & if\ C = 0 \\ \dfrac{G-B}{C} mod 6 & if\ M = R \\ \dfrac{B-R}{C} + 2 & if\ M = G \\ \dfrac{R-G}{C} + 4 & if\ M = B \end{cases} \tag{1}$$

$$H = 60^\circ \times H' \tag{2}$$

$$V = M \tag{3}$$

$$S = \begin{cases} 0 & ifV = 0 \\ \dfrac{C}{V} & otherwise \end{cases} \tag{4}$$

where $M = max(R, G, B)$, $m = min(R, G, B)$, $C = M - m$.

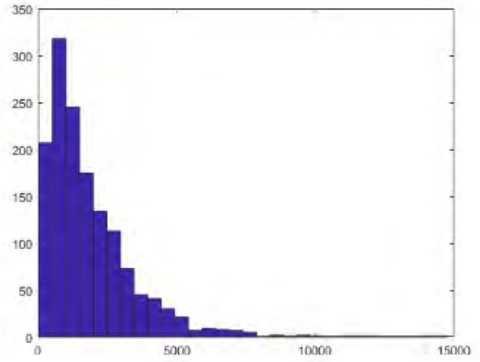

(a)

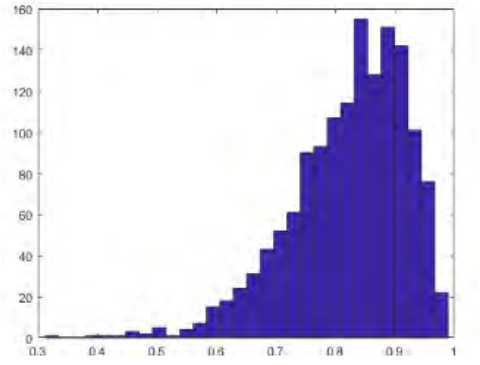

(b)

FIGURE 2. MSE and SSIM of NYU haze images in Hue channel. (a) MSE. (b) SSIM.

In [14], a dataset, D-HAZY, that contains more than one thousand pairs of images with ground truth reference images and hazy images of same scene is introduced. We calculate the MSE (mean square error) and SSIM (structural similarity index) between hue channels of hazy images and ground truth images. The results are shown in Fig.2. From Fig.2, we come to a conclusion that hazy images and haze-free images have similar hue. As for the brightness, we know from the scattering model that hazy images have higher pixel intensities. The saturation is then decreased.

Based on the analysis of the features of HSV color space, our proposed dehazing algorithm will only modify the saturation and brightness of the hazy images. For the intensity, we put forward a new algorithm, the modified morphological opening operation, to estimate the transmission map. For the saturation, we make full use of the relevance between the saturation and the brightness to derive the recovery coefficient. The flowchart of our algorithm is displayed in Fig.3.

B. INTENSITY RECOVERY BY OPENING OPERATION

We modify the traditional opening operation to apply it to the dark channel estimation. First, structuring elements used in dilation are set to be a little larger than structuring elements used in erosion. In this way, halo effect will be suppressed more significantly. Second, after opening, we limit the intensity to be smaller than the lowest value in three color channels.

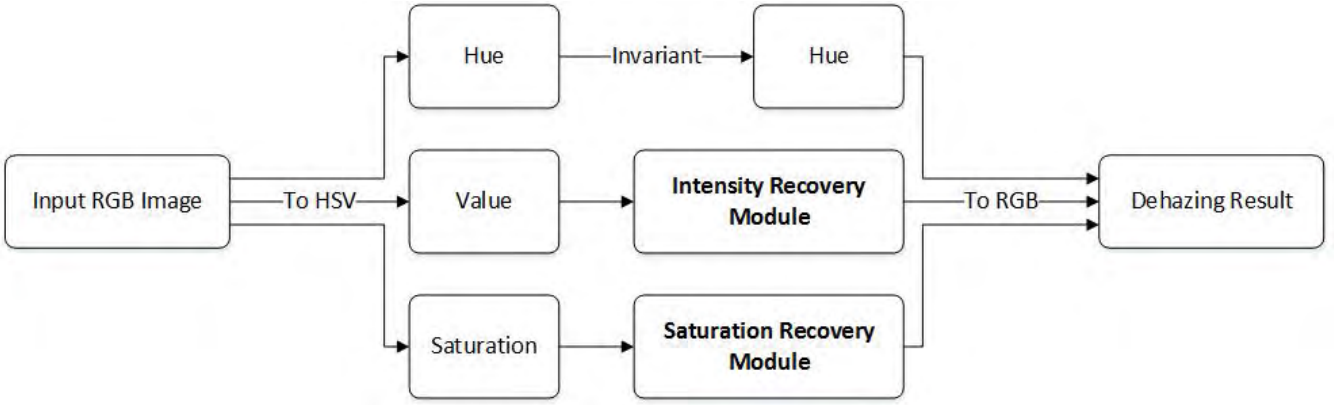

FIGURE 3. The flowchart of our algorithm.

This limitation is applied to avoid over correction in bright areas.

For an input RGB image I, we firstly calculate its minimum value in RGB channels:

$$I_{min}(x) = min_{c\in\{r,g,b\}} I^c(x) \tag{5}$$

Then we apply the proposed modified morphological opening operation to I_{min}. The shape of structuring elements (SE) is rectangle.

$$I_{erode}(x) = erode(I_{min}(x)), SE\ size(r_1, r_1) \tag{6}$$

$$I_{open}(x) = dilate(I_{erode}(x)), SE\ size(r_2, r_2) \tag{7}$$

$$I_{modify}(x) = min(I_{open}(x), I_{min}(x)) \tag{8}$$

Here, we use $I_{modify}(x)$ as the estimation of the dark channel. In our experiments, $r_2 = 35, r_1 = 31$. The values may vary based on the size of hazy images.

To obtain the global atmospheric light A, we pick the top 0.1% highest pixels from $I_{modify}(x)$ in consistent with [4]. Among them, pixel with the largest intensity in the V channel is selected as the atmospheric light.

Then, the transmission map $t(x)$ can be given as:

$$t(x) = 1 - \omega \frac{I_{modify}(x)}{A} \tag{9}$$

where ω is used to preserve distant haze, usually fixed as 0.9.

We use $t(x)$ and A to recover the value channel:

$$v^{recover}(x) = A + \frac{v(x) - A}{max(t(x), t_0)} \tag{10}$$

where $v(x)$ is the V channel of an input hazy image, t_0 is a user-defined lower bound.

After the opening operation, bright pixels in relatively dark areas will be replaced by neighboring pixels with the lowest intensity, and it has little impact on pixels in bright areas (usually more haze-occupied). Therefore, haze density in both dark areas and bright areas can be predicted by morphological opening results. Moreover, the edges of dark and bright areas will not be occupied by dark pixels because the followed dilation step will recover the edges. We use a larger structuring element for dilation to better suppress halo effects. Another advantage is that the opening eliminates texture fluctuations, thus making the dehazing result preserving more textures. Although the size of the structuring element is larger than the original dark channel algorithms which fix the window size as 15, we do not use computationally expensive filters so our algorithm is in fact more efficient than them.

C. SATURATION RECOVERY MODULE

Since the saturation is relevant to the brightness (4), we derive the recovery coefficient using the currently known intensity. For an arbitrary pixel p in hazy image, its RGB value is (R, G, B). Let M be the maximum of (R, G, B) and m be the minimum of (R, G, B). In HSV color space, the saturation of pixel p can be given by:

$$S = (M - m)/M \tag{11}$$

Suppose p in the output haze-free image has value (r, g, b). Using the scattering model, the new value can be expressed as:

$$new = A + \frac{old - A}{t(p)} \tag{12}$$

We can infer the recovered saturation:

$$S_{new} = \frac{M_{new} - m_{new}}{M_{new}} \tag{13}$$

where M_{new} is the maximum of (r, g, b) and m_{new} is the minimum of (r, g, b). Because the same restoration is used for each RGB color channel, the maximum and minimum values of a hazy image and a haze-free image are usually in the same channel. Thus, M_{new} and m_{new} can be given by:

$$M_{new} = A + \frac{M - A}{t(p)} m_{new} = A + \frac{m - A}{t(p)} \tag{14}$$

From (13) and (14), we derive that:

$$S_{new} = \frac{M - m}{M + A \times (t(p) - 1)} = S \times \frac{1}{1 + \frac{A \times (t(p) - 1)}{M}} \tag{15}$$

Here, we can use $\frac{1}{1+\frac{A\times(t(p)-1)}{M}}$ as a recovery coefficient to recover the saturation. Coincidentally, the maximum of input image does not need to be computed specially. The value channel in HSV color space is the maximum image of RGB. Moreover, the atmospheric light and transmission map are obtained when recovering intensity, thus making saturation recovery a quite time-saving step.

D. SUMMARY

In summary, the detailed algorithm is as follows:

Step 1: Apply opening operation. Given a hazy image I, we first apply the modified opening operation to its minimum value of RGB channels. The result serves as the estimated haze density.

Step 2: Convert I from RGB to HSV. Using the equation in section 2.1, we obtain the value channel and saturation channel.

Step 3: Estimate the atmospheric light. The atmospheric light A is picked as the brightest pixel of the value channel from the top 0.1% brightest pixels in I_{modify}.

Step 4: Apply the intensity recovery to the value channel. We have obtained the haze density estimation in step 1 and the atmospheric light in step 2, so the transmission map can be calculated using the atmospheric scattering model. Then, the value channel is recovered using (10).

Step 5: Apply the saturation recovery to the saturation channel. The saturation is closely relevant to the value channel, so we derive the equation using the value and transmission.

Step 6: Convert to RGB color space. The value and saturation are recovered through the recovery modules and the hue is invariant. After this, we can convert the image to RGB color space.

III. EXPERIMENTAL RESULTS

A. QUALITATIVE EVALUATION

We use D-HAZY dataset to evaluate our algorithm. The images in D-HAZY Middlebury are scaled to 1/4. Fig.4 shows some images in Middlebury dataset and their dehazing results. The names of these pictures are *Vintage*, *Bicycle*, *Backpack*, respectively. The result of Vintage demonstrates that our algorithm can achieve good result same as the guided filter DCP algorithm in smooth images. Our algorithm is better at avoiding color distortion. On the curtain area of the bicycle image, the significant color distortion is effectively suppressed by our algorithm. The halo effect in the backpack image has also been successfully erased using our algorithm while the traditional guided filter algorithm fails. Apart from He *et al.* [6], we also implement some latest proposed algorithms, including the light channel algorithm [15], DehazeNet [9], halo suppression algorithm [16] and surrogate modeling algorithm [10]. More comparisons are shown in Fig.5-7. In Fig.5, the color of trees and grass is well-preserved using our algorithm and the lake looks more natural. The mountain picture shows that our algorithm can suppress halo effects, thus preserving the edges. The results of the village picture indicates our algorithm preserve the naturalness of the trees in the distance.

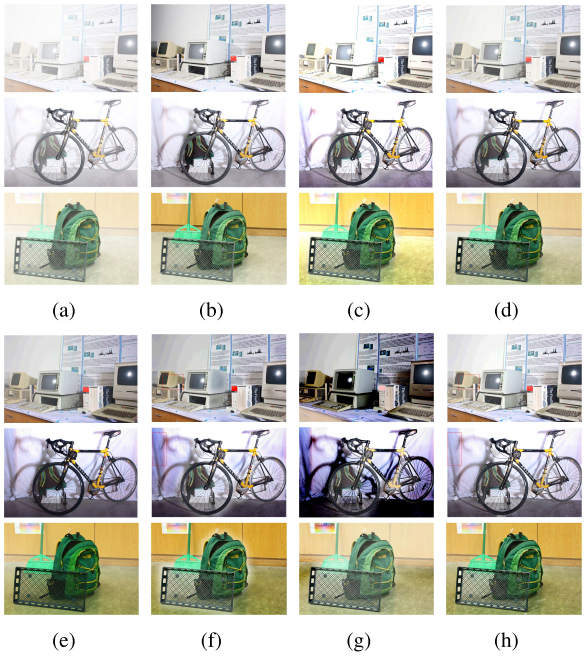

FIGURE 4. D-HAZY results. (a) Input images, (b) Ground truth, (c) Xu *et al.* [15], (d) Cai *et al.* [9], (e)Kim and Kang [16], (f) He *et al.* [6], (g) Jiang *et al.* [10] (h) Our HSV dehazing algorithm.

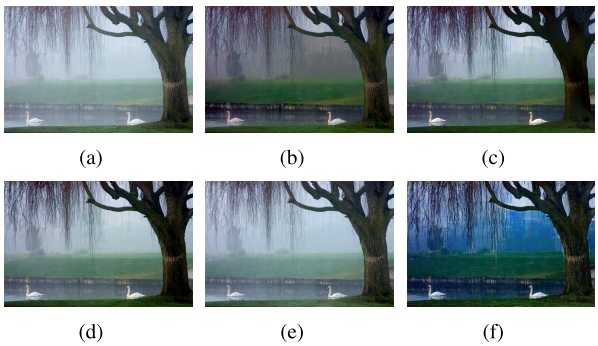

FIGURE 5. Swan. (a) Input image, (b) He *et al.* [6], (c) Zhu *et al.* [8], (d) Cai *et al.* [9], (e) Jiang *et al.* [10], (f) Our algorithm.

B. QUANTITATIVE EVALUATION

We compute SSIM and CIEDE2000 between ground truth images and dehazing results. The SSIM index compares local patterns of pixel intensities. The resulting SSIM index is a decimal value between -1 and 1, and value 1 is only reachable in the case of two identical sets of data. The color difference is measured by CIEDE2000, with values between 0 and 100. The smaller CIEDE2000 index means better color preservation. The results shown in Table 1 demonstrate that our algorithm is better at decreasing color difference. Without the halo effects and color distortion, our algorithm can preserve the naturalness of the haze-free images.

TABLE 1. Quantitative evaluation.

Images	He [6]		Xu [15]		Cai [9]		Kim [16]		Jiang [10]		Our Algorithm	
	SSIM	CIEDE	SSIM	CIEDE	SSIM	CIEDE	SSIM	CIEDE	SSIM	CIEDE	SSIM	CIEDE
Adirondack	0.84	10.02	0.81	15.55	0.84	12.00	0.83	9.46	0.679321	14.7314	**0.86**	**8.98**
Backpack	0.87	9.18	0.88	9.37	**0.89**	9.14	0.81	11.20	0.812759	11.1634	**0.89**	**7.83**
Bicycle1	0.79	12.74	0.91	6.32	**0.94**	**4.95**	0.84	13.89	0.568266	25.1158	0.87	10.67
Cable	0.64	17.10	0.58	39.17	0.62	27.64	0.62	22.19	0.540544	15.7958	**0.66**	**14.31**
Classroom1	**0.91**	8.46	0.70	23.82	0.70	22.23	0.79	10.66	0.689432	14.2961	0.85	**6.30**
Couch	**0.84**	**8.75**	0.62	17.83	0.59	21.10	0.68	10.74	0.496045	28.9464	0.71	9.31
Flowers	0.85	10.45	0.72	23.34	0.71	20.83	0.77	13.68	0.684878	12.1015	**0.86**	**7.13**
Jadeplant	**0.67**	22.40	0.54	34.48	0.52	30.40	0.61	**15.60**	0.474621	24.2916	0.60	19.66
Mask	0.81	**9.41**	0.85	13.41	**0.87**	10.47	0.82	11.74	0.732392	12.9015	0.86	**9.41**
Motorcycle	**0.80**	13.46	0.77	15.68	0.78	15.17	0.69	15.18	0.583854	18.1195	0.79	**13.11**
Piano	**0.86**	7.41	0.73	13.65	0.74	11.26	0.80	6.73	0.653797	14.8964	0.82	**6.72**
Pipes	**0.72**	11.82	0.62	23.91	0.64	18.64	0.63	12.70	0.378165	15.0906	0.70	**10.87**
Playroom	**0.86**	7.87	0.75	13.33	0.75	12.52	0.76	9.02	0.596577	17.2455	0.82	**7.00**
Playtable	**0.89**	**7.29**	0.84	12.78	0.84	12.21	0.82	9.03	0.750576	11.3454	0.88	7.60
Recycle	0.84	13.01	0.86	11.95	0.89	9.80	0.88	9.07	0.521972	31.4543	**0.89**	**8.43**
Shelves	**0.91**	7.24	0.87	11.59	0.88	7.28	0.83	10.21	0.851292	8.59429	0.89	**7.09**
Shopvac	0.64	17.35	0.54	34.52	0.58	30.41	0.64	22.43	0.633748	21.9561	**0.72**	**14.56**
Sticks	**0.95**	5.35	0.91	7.76	0.94	5.77	0.91	6.60	0.823709	12.0828	0.93	**4.77**
Storage	0.81	11.39	0.72	21.73	0.76	18.38	0.78	13.20	0.753254	13.226	**0.82**	**8.64**
Sword1	**0.88**	8.97	0.82	12.70	0.86	10.10	0.84	9.99	0.784408	12.7617	0.87	**7.74**
Sword2	0.83	10.90	0.80	17.37	0.85	14.14	0.87	10.29	0.745012	13.543	**0.88**	**9.96**
Umbrella	0.73	16.87	0.80	16.93	**0.88**	**11.39**	0.85	12.81	0.737929	16.524	0.84	12.63
Vintage	0.84	7.67	0.90	8.78	**0.95**	**5.47**	0.90	8.90	0.58465	23.949	0.91	6.41
Average	**0.82**	11.09	0.76	17.65	0.78	14.84	0.78	11.97	0.65553	16.9623	**0.82**	**9.53**

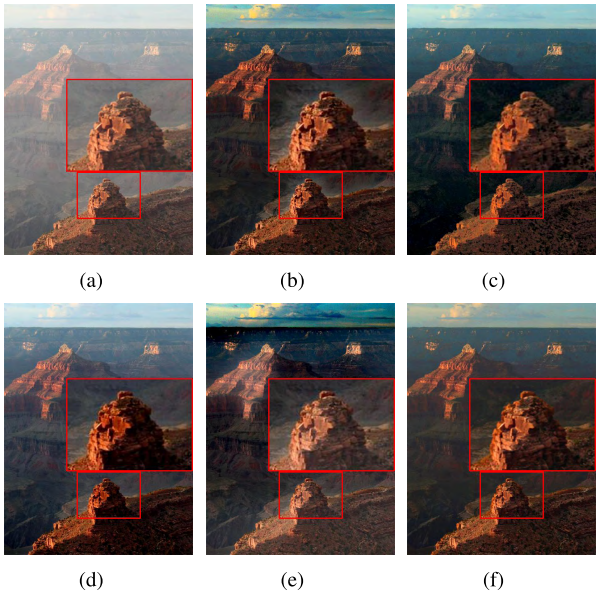

FIGURE 6. Mountain. (a)Input image, (b)He *et al.* [6], (c)Zhu *et al.* [8], (d) Cai *et al.* [9], (e) Jiang *et al.* [10], (f)Our algorithm.

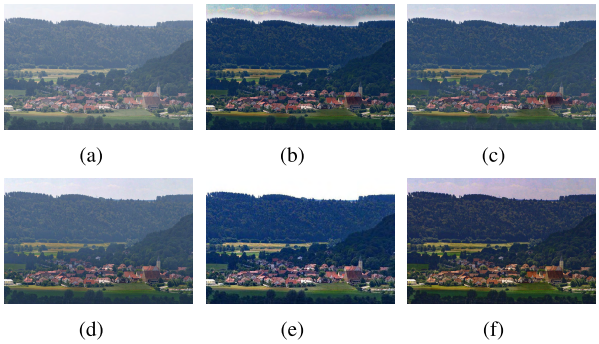

FIGURE 7. Village. (a)Input image, (b)He *et al.* [6], (c)Zhu *et al.* [8], (d) Cai *et al.* [9], (e) Jiang *et al.* [10], (f)Our algorithm.

C. COMPUTATION COMPLEXITY

As for time complexity, we test on D-HAZY NYU dataset. There are 1,449 hazy images with the same size 640×480. All of these algorithms are implemented on MATLAB R2017a.

TABLE 2. Time complexity comparison.

Function Name	Calls	Total Time	Time per image
guided_filter_dehaze [6]	1449	164.259 s	0.1131 s
halosuppression_dehaze [16]	1449	31.936 s	0.0213 s
lightchannel_dehaze [15]	1449	291.456 s	0.2008 s
DehazeNet [9]	1449	5698.203 s	3.9323 s
hsv_dehaze(Our)	1449	86.764 s	0.0593 s

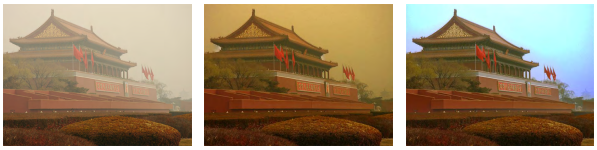

FIGURE 8. (a)Input Image, (b)Our dehazing result, (c)Our result after white balance.

The time reported here is from MATLAB profiler tool. The CPU platform is Intel Core i5-7300HQ with 8G RAM. From Table 2, we can see that the refinement step "guidedfilter" is very time consuming. It is mainly because the "boxfilter" function will be called seven times for one image. In fact, box filter improves efficiency comparing to mean filter. But it is still the bottleneck of guided filter. In contrast, the proposed algorithm reduces time complexity by 47.1%, which is a significant gain. Based on MATLAB profiler analysis result, the most time consuming part of the proposed algorithm is color space converting. The light channel algorithm [15] will be as fast as guided filter DCP algorithm with parallel processing. Without parallel processing, it will be slower. The halo effect suppression algorithm [16] is the fastest because it uses a simple coefficient to refine the transmission map. Therefore, their transmission maps are the most unprecise. DehazeNet [9] is very time-consuming because it uses a complex neural network.

IV. CONCLUSION

In this paper,we propose a naturalness preserved fast algorithm for single image dehazing. Our proposed algorithm can

effectively suppress halo effects by applying the modified opening operation to estimate the transmission map. In the meantime, we avoid color distortion through the HSV color space. It is consistent with observed conditions to enhance the visibility of hazy images in HSV color space. Also, the time complexity has been reduced significantly. Experimental results demonstrate that our algorithm outperforms other algorithms both visually and quantitatively.

In spite of this, our algorithm is still unable to recover the visually satisfied color for images captured in complex weather conditions like sandstorm. The atmospheric light is no longer white in these situations, so white balance methods, such as gray world method, perfect reflector method and fuzzy rules method [17], are necessary(Fig.8).

REFERENCES

[1] S. K. Nayar and S. G. Narasimhan, "Vision in bad weather," in *Proc. IEEE 7th Conf. Comput. Vis.*, vol. 2. Sep. 1999, pp. 820–827.
[2] R. T. Tan, "Visibility in bad weather from a single image," in *Proc. IEEE Conf. Comput. Vis. Pattern Recognit. (CVPR)*, Jun. 2008, pp. 1–8.
[3] R. Fattal, "Single image dehazing," *ACM Trans. Graph.*, vol. 27, no. 3, p. 72, 2008.
[4] K. He, J. Sun, and X. Tang, "Single image haze removal using dark channel prior," in *Proc. IEEE Conf. Comput. Vis. Pattern Recognit. (CVPR)*, Dec. 2009, pp. 1956–1963.
[5] S.-C. Huang, B.-H. Chen, and W.-J. Wang, "Visibility restoration of single hazy images captured in real-world weather conditions," *IEEE Trans. Circuits Syst. Video Technol.*, vol. 24, no. 10, pp. 1814–1824, Oct. 2014.
[6] K. He, J. Sun, and X. Tang, "Guided image filtering," *IEEE Trans. Pattern Anal. Mach. Intell.*, vol. 35, no. 6, pp. 1397–1409, Jun. 2013.
[7] Y.-Q. Zhang, Y. Ding, J.-S. Xiao, J. Liu, and Z. Guo, "Visibility enhancement using an image filtering approach," *EURASIP J. Adv. Signal Process.*, vol. 2012, no. 1, p. 220, 2012.
[8] Q. Zhu, J. Mai, and L. Shao, "Single image dehazing using color attenuation prior," in *Proc. Brit. Mach. Vis. Conf.*, 2014. [Online]. Available: http://www.bmva.org/bmvc/2014/papers/paper111/index.html
[9] B. Cai, X. Xu, K. Jia, C. Qing, and D. Tao, "DehazeNet: An end-to-end system for single image haze removal," *IEEE Trans. Image Process.*, vol. 25, no. 11, pp. 5187–5198, Nov. 2016.
[10] Y. Jiang, C. Sun, Y. Zhao, and L. Yang, "Fog density estimation and image defogging based on surrogate modeling for optical depth," *IEEE Trans. Image Process.*, vol. 26, no. 7, pp. 3397–3409, Jul. 2017.
[11] Y. Gao, H.-M. Hu, B. Li, and Q. Guo, "Naturalness preserved nonuniform illumination estimation for image enhancement based on retinex," *IEEE Trans. Multimedia*, vol. 20, no. 2, pp. 335–344, Feb. 2018.
[12] Y. Gao, H.-M. Hu, S. Wang, and B. Li, "A fast image dehazing algorithm based on negative correction," *Signal Process.*, vol. 103, pp. 380–398, Oct. 2014.
[13] Y. Wan and Q. Chen, "Joint image dehazing and contrast enhancement using the HSV color space," in *Proc. Vis. Commun. Image Process.*, 2016, pp. 1–4.
[14] C. Ancuti, C. O. Ancuti, and C. De Vleeschouwer, "D-HAZY: A dataset to evaluate quantitatively dehazing algorithms," in *Proc. IEEE Int. Conf. Image Process.*, Sep. 2016, pp. 2226–2230.
[15] Y. Xu, X. Guo, H. Wang, F. Zhao, and L. Peng, "Single image haze removal using light and dark channel prior," in *Proc. IEEE/CIC Int. Conf. Commun. China (ICCC)*, Jul. 2016, pp. 1–6.
[16] G.-J. Kim and B. Kang, "Halo effect suppression for single image haze removal method," in *Proc. Int. SoC Design Conf. (ISOCC)*, Oct. 2016, pp. 323–324.
[17] Y.-C. Liu, W.-H. Chan, and Y.-Q. Chen, "Automatic white balance for digital still camera," *IEEE Trans. Consum. Electron.*, vol. 41, no. 3, pp. 460–466, Aug. 1995.

TIANYU ZHANG received the B.S. degree in computer science and technology from Beihang University, Beijing, China, in 2017, where he is currently pursuing the Ph.D. degree in computer science and technology.

His research interests include computer vision, image processing, pattern recognition, and machine learning.

HAI-MIAO HU received the B.S. degree in computer science from Central South University, Changsha, China, in 2005, and the Ph.D. degree in computer science from Beihang University, Beijing, China, in 2012. He was a Visiting Student with the University of Washington from 2008 to 2009.

He is currently an Associate Professor of computer science and engineering with Beihang University. His research interests include video coding and networking, image/video processing, and video analysis and understanding.

BO LI received the B.S. degree in computer science from Chongqing University in 1986, the M.S. degree in computer science from Xi'an Jiaotong University in 1989, and the Ph.D. degree in computer science from Beihang University in 1993.

He is currently a Professor of computer science and engineering with Beihang University, where he is also the Director of the Beijing Key Laboratory of Digital Media. He has authored over 100 conference and journal papers in diversified research fields, including digital video and image compression, video analysis and understanding, remote sensing image fusion, and embedded digital image processor.